

f_K/f_π in full QCD with domain wall valence quarksS. R. Beane,^{1,2} P. F. Bedaque,^{3,4} K. Orginos,^{2,5} and M. J. Savage⁶

(NPLQCD Collaboration)

¹*Department of Physics, University of New Hampshire, Durham, New Hampshire 03824-3568, USA*²*Jefferson Laboratory, 12000 Jefferson Avenue, Newport News, Virginia 23606, USA*³*Department of Physics, University of Maryland, College Park, Maryland 20742-4111, USA*⁴*Lawrence-Berkeley Laboratory, Berkeley, California 94720, USA*⁵*Department of Physics, College of William and Mary, Williamsburg, Virginia 23187-8795, USA*⁶*Department of Physics, University of Washington, Seattle, Washington 98195-1560, USA*

(Received 16 August 2006; published 2 May 2007)

We compute the ratio of pseudoscalar decay constants f_K/f_π using domain-wall valence quarks and rooted improved Kogut-Susskind sea quarks, at a lattice spacing of $b \sim 0.125$ fm. By employing continuum chiral perturbation theory, we extract the Gasser-Leutwyler low-energy constant L_5 and extrapolate f_K/f_π to the physical point. We find $f_K/f_\pi = 1.218 \pm 0.002_{-0.024}^{+0.011}$ where the first error is statistical and the second error is an estimate of the systematic due to chiral extrapolation and fitting procedures. This value agrees within the uncertainties with the determination by the MILC collaboration, calculated using Kogut-Susskind valence quarks, suggesting that systematic errors arising from the choice of lattice valence quark are small.

DOI: [10.1103/PhysRevD.75.094501](https://doi.org/10.1103/PhysRevD.75.094501)

PACS numbers: 11.15.Ha, 11.30.Rd, 12.38.Aw, 12.38.-t

I. INTRODUCTION

Recently, lattice QCD calculations have been quite successful in determining the hadronic matrix elements and low-energy constants required for precisely extracting Cabibbo-Kobayashi-Maskawa (CKM) matrix elements, such as V_{bc} and V_{us} , from experimental data [1–7]. In particular, lattice determinations of the pseudoscalar decay constants [1] f_K and f_π , when combined with the experimentally measured branching fractions for $K \rightarrow \mu \bar{\nu}_\mu(\gamma)$ and $\pi \rightarrow \mu \bar{\nu}_\mu(\gamma)$, provide important theoretical input into establishing the value of V_{us} [3], the charged-current matrix element for $s \rightarrow u$ transitions. Precise determinations of V_{us} and V_{ud} , together with the fact that the square of V_{ub} is negligibly small, provide for a clean test of the unitarity of the CKM matrix, and therefore facilitate a low-energy probe for physics beyond the standard model with three generations of quarks.

Recent developments in improving the Kogut-Susskind (KS) action [8–13] have allowed for the computation of quantities in full QCD, with two light and one strange dynamical quark flavors [14], near the physical point. Although such calculations currently represent the most accurately calculated predictions of QCD, one should keep in mind that there may be uncontrolled errors due to the fact that KS fermions naturally appear with four copies (tastes). In order to use them in computations with one or two flavors, one must take fractional powers of the KS fermionic determinant, which may lead to errors arising from nonlocalities. While this problem remains under investigation, there exists significant evidence that, in practice, this procedure is benign. The low-energy effective

field theories describing quantities computed on the lattice with KS fermions which are used to perform chiral and continuum extrapolations, and also to determine finite-volume effects, are complicated by the taste structure, which introduces new low-energy constants [15,16] beyond those that appear in the low-energy effective field theory of QCD. Using the LHPC mixed-action calculational scheme [17,18], one can alleviate the above-mentioned problems, as flavor symmetry and chiral symmetry (up to exponentially small corrections) can be preserved in the valence sector by the use of domain-wall fermions [19–23]. Even in this scheme, the finite lattice-spacing corrections due to the sea of KS fermions are involved [24,25], but they are $O(g^2 b^2)$ (where g is the QCD coupling constant and b is the lattice spacing) and in some cases they may be negligible as was observed in the case of $I = 2$ $\pi\pi$ scattering [26] and the more recent exploration of the Gell-Mann-Okubo relation for octet baryons [27], and calculation of the strong isospin breaking in the nucleon [28].

In the calculation described here, we use the MILC rooted KS 2 + 1 dynamical fermion lattices [11,13,14,29] at a lattice spacing of $b \sim 0.125$ fm and domain-wall valence quarks [19–23] to compute the pseudoscalar decay constants f_K and f_π , and, in particular, the ratio of the two. As any deviation from unity in the ratio of the decay constants results from the breaking of $SU(3)$ flavor symmetry, contributions from finite lattice spacing must be accompanied by $SU(3)$ breaking quantities, and therefore are suppressed beyond the naive $O(g^2 b^2)$. It follows that it is appropriate to employ continuum $SU(3)$ chiral perturbation theory to extrapolate the lattice data to

TABLE I. The parameters of the MILC gauge configurations and domain-wall propagators used in this work. The subscript l denotes the light quark (up and down), and s denotes the strange quark. The superscript dwf denotes the bare quark mass for the domain-wall fermion propagator calculation. The last column is the number of configurations times the number of sources per configuration.

Ensemble	bm_l	bm_s	bm_l^{dwf}	bm_s^{dwf}	$10^3 \times bm_{\text{res}}^a$	# of propagators
2064f21b676m007m050	0.007	0.050	0.0081	0.081	1.604 ± 0.038	468×3
2064f21b676m010m050	0.010	0.050	0.0138	0.081	1.552 ± 0.027	658×4
2064f21b679m020m050	0.020	0.050	0.0313	0.081	1.239 ± 0.028	486×3
2064f21b681m030m050	0.030	0.050	0.0478	0.081	0.982 ± 0.030	564×3

^aComputed by the LHP collaboration.

the physical values of the light-quark masses, and to make a prediction for f_K/f_π . This calculation provides an important test of the systematics involved in the earlier calculations of the same quantity by MILC [1,2]. Significant differences between the two extrapolations would indicate an uncontrolled systematic associated with the species of valence quarks employed in the calculation. In this paper we obtain a result that is consistent with the MILC result, and, consequently, we find no evidence of a significant systematic error in the lattice calculation of f_K/f_π due to finite lattice-spacing effects.

II. DETAILS OF THE LATTICE CALCULATION

Our computation uses the mixed-action lattice QCD scheme developed by LHPC [17,18] using domain-wall valence quarks from a smeared source on $N_f = 2 + 1$ asqtad-improved [11,13] MILC configurations generated with rooted¹ KS sea quarks [14] that are hypercubic smeared (HYP smeared) [38–41]. In the generation of the MILC configurations, the strange-quark mass was fixed near its physical value, $bm_s = 0.050$ (where $b \sim 0.125$ fm is the lattice spacing²), determined by the mass of hadrons containing strange quarks. The two light quarks in the configurations are degenerate (isospin symmetric). As was shown by LHPC [17,18], HYP smearing allows for a significant reduction in the residual chiral symmetry breaking at a moderate extent $L_s = 16$ of the extra dimension and domain-wall height $M_5 = 1.7$. In order to reduce the time required for propagator generation by a factor of 2, the time direction of MILC lattices was reduced by a factor of 2, from 64 down to 32. As the gauge fields are no longer antiperiodic in the time direction, a Dirichlet boundary condition is imposed on the propagator in the time direction, while retaining periodic boundary conditions in the spatial directions. This also allowed us to recycle propagators computed for the nucleon structure function calcu-

lations performed by LHPC. The impact of the Dirichlet boundary condition on correlation functions falls exponentially with the distance in the time direction to the boundary and did not restrict the extraction of physics from the calculation. For bare domain-wall fermion masses we used the tuned values that match the KS Goldstone pion to few-percent precision. For details of the matching see Refs. [17,18]. The parameters used in the propagator calculation are summarized in Table I. All propagator calculations were performed using the CHROMA software suite [42,43] on the high-performance computing systems at the Jefferson Laboratory (JLab).

In order to be able to extract the pseudoscalar decay constants from the amplitude of the pseudoscalar correlators, $C_P(t)$, as was done in [44,45], both the smeared-smeared and smeared-point pseudoscalar correlation functions are computed. If the amplitudes of the pseudoscalar ground state are $\mathcal{A}_P^{\text{ss}}$ and $\mathcal{A}_P^{\text{sp}}$ for the smeared-smeared and smeared-point correlators, respectively, the pseudoscalar decay constant is recovered from

$$f_P = \frac{\mathcal{A}_P^{\text{sp}}}{\sqrt{\mathcal{A}_P^{\text{ss}}}} \frac{\sqrt{2}(m_1^{\text{dwf}} + m_2^{\text{dwf}} + 2m_{\text{res}})}{m_P^{3/2}} \quad (1)$$

where m_1^{dwf} and m_2^{dwf} are the domain-wall fermion masses used in constructing the pseudoscalar meson and m_{res} is the residual chiral symmetry breaking parameter computed from the chiral Ward-Takahashi identity as in [44,45] and shown in Table I. The dependence of m_{res} on the valence mass is negligible compared to the statistical errors of the calculation. It is useful to construct an “effective” decay constant directly from the lattice data at each time slice. Hence we form

$$f_P^{\text{EFF}} = \frac{C_P^{\text{SP}}(t)^{t+1} C_P^{\text{SS}}(t+1)^{t/2}}{C_P^{\text{SS}}(t)^{(t+1)/2} C_P^{\text{SP}}(t+1)^t} \times \frac{\sqrt{2}(m_1^{\text{dwf}} + m_2^{\text{dwf}} + 2m_{\text{res}})}{[\log(C_P^{\text{SP}}(t)C_P^{\text{SP}}(t+1)^{-1})]^{3/2}}, \quad (2)$$

which is independent of t at large times where the correlation functions behave as

$$C_P^{\text{SP}}(t) \rightarrow \mathcal{A}_P^{\text{sp}} e^{-m_P t}, \quad C_P^{\text{SS}}(t) \rightarrow \mathcal{A}_P^{\text{ss}} e^{-m_P t}. \quad (3)$$

¹For recent discussions of the “legality” of the mixed-action and rooting procedures, see Refs. [30–37].

²The lattice spacing has been determined to be [1] $b = 0.1243 \pm 0.0015$ fm using the Sommer scale-setting procedure, and [26] $b = 0.1274 \pm 0.0007 \pm 0.0003$ fm using the pion decay constant. In this work quantities in physical units were obtained using $b = 0.125$ fm.

III. ANALYSIS AND CHIRAL EXTRAPOLATION

To determine the pseudoscalar decay constants, the correlation functions for the K^+ and π^+ were computed with both smeared and point sinks on each ensemble. In order to extract the amplitudes for the smeared-smeared and smeared-point correlation functions, a single exponential³ with a common mass was fit by χ^2 minimization to each data set, i.e. a three parameter fit was performed with variables \mathcal{A}_p^{ss} , \mathcal{A}_p^{sp} and m_π (or m_K). The central value and uncertainty of each parameter were determined by the jackknife procedure over the ensemble of configurations. The decay constant was extracted by jackknifing over the appropriate combination of quantities, as given in Eq. (1). In Fig. 1 we present the lattice data using effective f_K/f_π plots according to Eq. (2), along with the fits. The results of the lattice calculation of the decay constants and meson masses are tabulated in Table II.

A. Chiral extrapolation at next-to-leading order

In $SU(3)$ chiral perturbation theory (χ PT) Gasser and Leutwyler [48–50] showed that the ratio of the kaon to pion decay constants is given, at next-to-leading order (NLO) in the chiral expansion, by

$$\frac{f_K}{f_\pi} = 1 + \frac{5}{4}l_\pi(\mu) - \frac{1}{2}l_K(\mu) - \frac{3}{4}l_\eta(\mu) + \frac{8}{f^2}(m_K^2 - m_\pi^2)L_5(\mu) \quad (4)$$

where f is the pseudoscalar decay constant in the chiral limit, m_K is the kaon mass, m_π is the pion mass, and

$$l_i(\mu) \equiv \frac{1}{16\pi^2} \frac{m_i^2}{f^2} \log\left(\frac{m_i^2}{\mu^2}\right), \quad (5)$$

with the index i running over the pseudoscalar states (π , K , and η). $L_5(\mu)$ is a Gasser-Leutwyler low-energy constant evaluated at the χ PT renormalization scale μ , whose scale dependence exactly compensates the scale dependence of the logarithmic contributions.

In our lattice calculation we have not computed the mass of the η meson since it involves disconnected diagrams that require significant computer time to evaluate. Hence we replace m_η with its value obtained from the Gell-Mann-Okubo mass relation among octet mesons,

$$m_\eta^2 = \frac{4}{3}m_K^2 - \frac{1}{3}m_\pi^2, \quad (6)$$

which is valid to the order of χ PT to which we are working.

³There is no evidence of excited state contamination in the π -correlation function, determined by performing double exponential fits to the data, from time-slice 4 onward. While one expects a contribution from 3π and π^* intermediate states at short times [46,47], we were unable to extract a mass for such states.

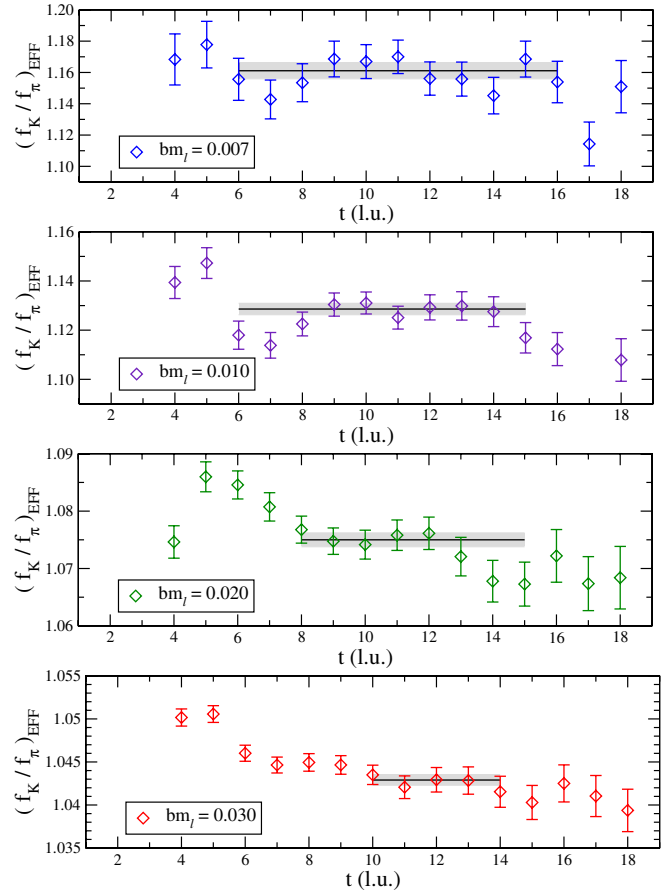


FIG. 1 (color online). Effective f_K/f_π determined from the smeared-smeared and smeared-point correlation functions with Eq. (2). The solid black lines and shaded regions are the fits (with 1σ errors) tabulated in Table II.

In addition, we choose to work with $\mu = f_\pi^{\text{phy}}$, the value of the pion decay constant at the physical point. To recover the value of the counterterm $L_5(\mu)$ at some other renormalization scale, one can use the evolution [48–50]

$$L_5(f_\pi^{\text{phy}}) = L_5(\mu) - \frac{3}{8} \frac{1}{16\pi^2} \log\left(\frac{f_\pi^{\text{phy}}}{\mu}\right). \quad (7)$$

Finally, we replace the ratios $(m_i/f_\pi^{\text{phy}})^2$ by the lattice-computed value $(m_i/f_\pi)^2$, which is again consistent to the order of χ PT to which we are working. Hence, the final NLO expression to which we fit the lattice data is

$$\begin{aligned} \frac{f_K}{f_\pi} = & 1 + \frac{5}{4} \frac{1}{16\pi^2} \frac{m_\pi^2}{f_\pi^2} \log\left(\frac{m_\pi^2}{f_\pi^2}\right) - \frac{1}{2} \frac{1}{16\pi^2} \frac{m_K^2}{f_\pi^2} \log\left(\frac{m_K^2}{f_\pi^2}\right) \\ & - \frac{1}{16\pi^2} \left(\frac{m_K^2}{f_\pi^2} - \frac{1}{4} \frac{m_\pi^2}{f_\pi^2}\right) \log\left(\frac{4}{3} \frac{m_K^2}{f_\pi^2} - \frac{1}{3} \frac{m_\pi^2}{f_\pi^2}\right) \\ & + 8 \left(\frac{m_K^2}{f_\pi^2} - \frac{m_\pi^2}{f_\pi^2}\right) L_5(f_\pi^{\text{phy}}). \end{aligned} \quad (8)$$

Note that the only parameter to be determined by fitting at

TABLE II. Calculated quantities with fitting ranges in brackets. All errors are computed using the jackknife procedure. Values for \mathcal{F} are given without and with (in squiggly brackets) the \log^2 contribution.

Ensemble	m_π (GeV)	m_π/f_π	m_K/f_π	f_K/f_π	$\mathcal{F} \times 10^3$
m007	0.2931(15)	1.978(19) [5–16]	3.937(28) [6–16]	1.1610(54) [6–16]	5.67(6) {5.31(5)}
m010	0.3546(9)	2.337(11) [5–16]	3.958(16) [6–15]	1.1286(23) [6–15]	5.62(3) {5.13(2)}
m020	0.4934(12)	3.059(12) [7–16]	3.988(15) [7–15]	1.0751(13) [8–15]	5.68(3) {4.87(2)}
m030	0.5918(10)	3.484(10) [5–15]	4.004(12) [7–14]	1.04279(69) [10–14]	5.73(2) {4.69(2)}

NLO is L_5 . It is also worth noting that the above expression has the expected behavior that at the $SU(3)$ symmetric point the ratio of decay constants is unity.

For reasons that will become clear below, it is useful to “linearize” the fitting procedure by isolating the analytic terms with coefficients that are to be fit to the lattice data. We define the function

$$\mathcal{F} \equiv \left(\frac{f_K}{f_\pi} - 1 - \chi_{\log s} \right) \frac{1}{8y}, \quad (9)$$

where, at NLO,

$$\begin{aligned} \chi_{\log s} &= \chi_{\log s}^{(\text{NLO})} \left(\frac{m_\pi}{f_\pi}, \frac{m_K}{f_\pi} \right) \\ &= \frac{5}{4} \frac{1}{16\pi^2} \frac{m_\pi^2}{f_\pi^2} \log \left(\frac{m_\pi^2}{f_\pi^2} \right) - \frac{1}{2} \frac{1}{16\pi^2} \frac{m_K^2}{f_\pi^2} \log \left(\frac{m_K^2}{f_\pi^2} \right) \\ &\quad - \frac{1}{16\pi^2} \left(\frac{m_K^2}{f_\pi^2} - \frac{1}{4} \frac{m_\pi^2}{f_\pi^2} \right) \log \left(\frac{4}{3} \frac{m_K^2}{f_\pi^2} - \frac{1}{3} \frac{m_\pi^2}{f_\pi^2} \right), \end{aligned} \quad (10)$$

and the quantity y is

$$y = \frac{m_K^2}{f_\pi^2} - \frac{m_\pi^2}{f_\pi^2}. \quad (11)$$

Therefore, at NLO in the chiral expansion, the quantity \mathcal{F} should be the same on each of the ensembles, and equal to the counterterm $L_5(f_\pi^{\text{phy}})$,

$$\mathcal{F} = L_5(f_\pi^{\text{phy}}). \quad (12)$$

The calculated values of \mathcal{F} , along with their uncertainties determined by jackknifing over the configurations, are shown in Table II, and in Fig. 2 we have plotted \mathcal{F} versus m_π^2/f_π^2 . A χ^2 minimization is performed to extract the one parameter $L_5(f_\pi^{\text{phy}})$ from the data. The complete lattice data set is not that well described by a constant value of $L_5(f_\pi^{\text{phy}})$, “Fit A” in Fig. 2, due to the presence of higher-order terms in the chiral expansion, or failure of the chiral expansion at the highest pion mass. To explore the dependence on the higher-order terms in the chiral expansion we have sequentially “pruned” the data by removing the highest mass point ($bm_l = 0.030$), and then the two highest mass points ($bm_l = 0.030, 0.020$), and

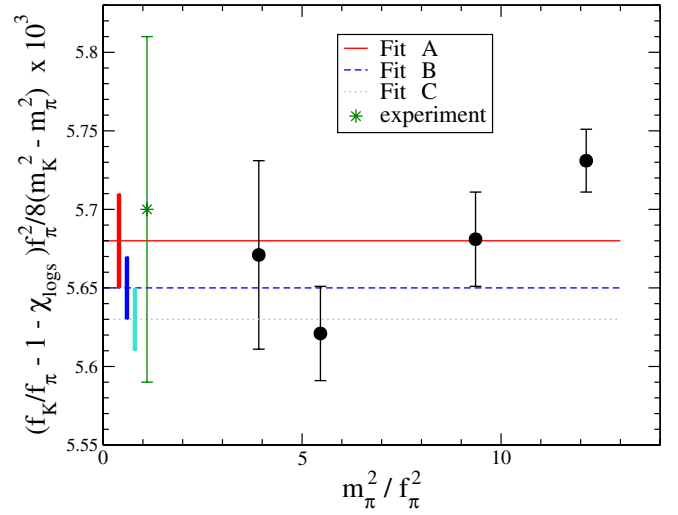


FIG. 2 (color online). \mathcal{F} vs m_π^2/f_π^2 at NLO, along with the three different fits, A, B and C. The solid bars near the y axis denote the value of L_5 and its uncertainty from the three fits. The point denoted by the star corresponds to the experimental value.

determined $L_5(f_\pi^{\text{phy}})$,⁴ “Fit B” and “Fit C” in Fig. 2, respectively. The results of these fits are shown in Fig. 2 and presented in Table III. With the value of L_5 , we use Eq. (8) to evaluate the ratio of the decay constants at the physical point using the physical values for the pseudoscalar masses and the pion decay constant [51],

$$\begin{aligned} f_{\pi^+} &= 130.7 \text{ MeV}, & m_\pi &= 137.3 \text{ MeV}, \\ m_K &= 495.7 \text{ MeV}, \end{aligned} \quad (13)$$

where the masses are the isospin-averaged values. We use the Gell-Mann-Okubo mass relation to determine the η mass that appears in the chiral contributions.

It is important to keep in mind that this determination of L_5 is only perturbatively close to the actual value of L_5

⁴Pruning the data provides an assessment of the importance of higher-order terms in the chiral expansion, while fitting only the leading chiral contributions. There are a number of ways to approach this issue. For instance, an alternate approach would be to add a systematic error to each data point that grows with the pion mass in a manner consistent with χ PT. We find that this provides an extrapolated value of f_K/f_π and L_5 consistent with pruning the data, as expected.

TABLE III. Results from chiral extrapolation at one-loop order in χ PT. Explanations of the various fits are in the text.

Fit	$L_5 \times 10^3$	f_K/f_π (extrapolated)	χ^2/dof
A	5.68(3)	1.221(3)	3.5
B	5.65(2)	1.218(2)	1.4
C	5.63(2)	1.215(2)	0.7

which is defined in the chiral limit. In the current extraction, the strange-quark mass is held fixed near the physical value, while the light-quark masses are somewhat lighter.

B. Incomplete chiral extrapolations at next-to-next-to-leading order

While the full two-loop expressions for f_K/f_π exist in both QCD [52] and partially quenched QCD [53], these expressions contain many fit parameters, and therefore fruitful use of these results must await lattice data with better statistics and with a larger variety of quark masses. In order to estimate systematic errors, we perform fits with parts of the next-to-next-to-leading-order (NNLO) expression [54]. We focus on just two of the structures that enter at NNLO, analytic terms and a double logarithm with fixed coefficient.

1. Partial N²LO: Analytic terms only

Including only the analytic terms that enter at NNLO, Eq. (12) becomes

$$\mathcal{F} = L_5 + C_s m_s + C_l m_l = \tilde{L}_5 + \tilde{C}_\pi \frac{m_\pi^2}{f_\pi^2}, \quad (14)$$

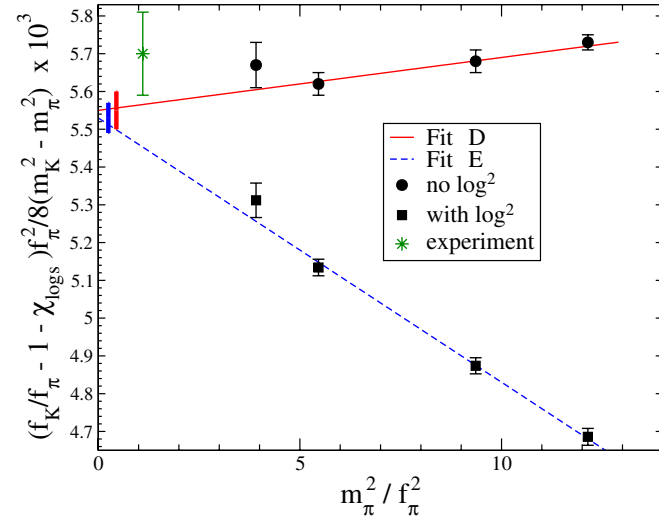


FIG. 3 (color online). \mathcal{F} vs m_π^2/f_π^2 at NNLO. The solid bars near the y axis denote the value of $\tilde{L}_5 = \mathcal{F}(m_\pi = 0)$ and its uncertainty from the fits. The point denoted by the star corresponds to the experimental value. The circles denote the lattice data with only the NLO chiral logs subtracted, while the squares are the lattice data with the NLO chiral logs and the NNLO \log^2 term subtracted.

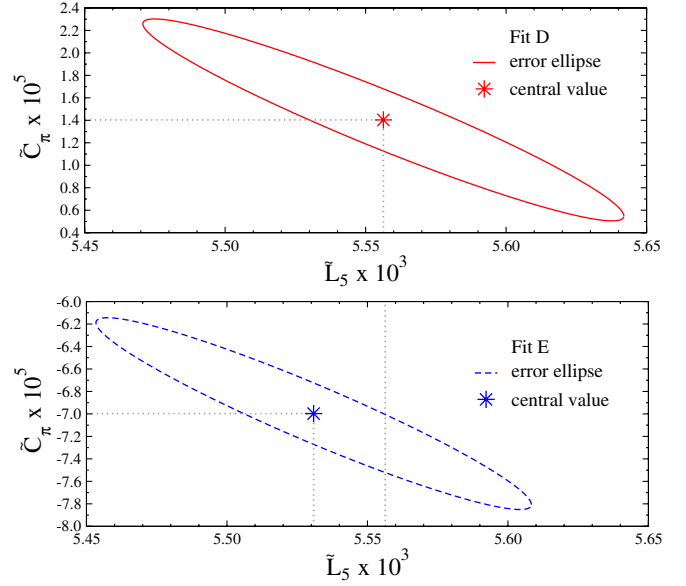


FIG. 4 (color online). 68% confidence-level error ellipses for fits D and E described in the text.

TABLE IV. Results from fitting the partial NNLO chiral contributions. Explanations of fits D, E, F, and G are in the text.

Fit	$\tilde{L}_5 \times 10^3$	$\tilde{C}_\pi \times 10^5$	f_K/f_π (extrapolated)	χ^2/dof
D	5.63(2)	1.40(49)	1.209(8)	0.8
E	5.53(4)	-7.00(47)	1.209(7)	1.0
F	5.80(3)	-8.28(35)	1.224(5)	0.5
G	5.16(5)	-4.93(56)	1.205(9)	1.5

where terms higher order in the chiral expansion are not shown. As the strange-quark mass is the same over all ensembles, we simply absorb it into the definition of L_5 , making explicit the quark mass dependence discussed previously. Therefore fitting at NNLO holding the strange-quark mass fixed introduces one additional fit parameter, \tilde{C}_π . It is clear that the values of \tilde{L}_5 and \tilde{C}_π extracted from the data are correlated, and in determining the extrapolated value of f_K/f_π we explore the entire 68% confidence-level error ellipse in the $\tilde{L}_5 - \tilde{C}_\pi$ plane⁵ (shown in Fig. 4). We label this “Fit D,” and the results are shown in Table IV. The data minus the NLO chiral logs, and the fit are shown in Fig. 3. Note that the errors quoted in Table IV and displayed in Fig. 3 are 1σ errors.

2. Partial N²LO: Analytic terms and double chiral logs

The full two-loop expression that contributes to f_K/f_π is quite complicated. An approximation to the \log^2 piece at two-loop order can be evaluated using renormalization-

⁵This results in an error that is consistent with textbook propagation of the errors in \tilde{L}_5 and \tilde{C}_π .

group techniques and is given by [54]

$$\chi_{\log^2}^{(\text{NNLO})} = \frac{1}{6144\pi^4} \left(\frac{m_K^2}{f_\pi^2} - \frac{m_\pi^2}{f_\pi^2} \right) \left(17 \frac{m_K^2}{f_\pi^2} + 37 \frac{m_\pi^2}{f_\pi^2} \right) \times \log^2 \left(\frac{M^2}{\mu^2} \right), \quad (15)$$

where M is a mass scale related to the Goldstone boson masses. It would seem reasonable to choose the intermediate mass scale $M = \sqrt{m_\pi m_K}$ and $\mu = f_\pi$. Of course, the two-loop contributions vanish at the flavor $SU(3)$ symmetric point. Again, to isolate the fitting function, we subtract $\chi_{\log^2}^{(\text{NNLO})}$ from the lattice data, giving a fit function of the form

$$\begin{aligned} \mathcal{F} &\equiv \left(\frac{f_K}{f_\pi} - 1 - \chi_{\log^2}^{(\text{NLO})} - \chi_{\log^2}^{(\text{NNLO})} \right) \frac{1}{8y} \\ &= \tilde{L}_5(f_\pi^{\text{phy}}) + \tilde{C}_\pi \frac{m_\pi^2}{f_\pi^2}. \end{aligned} \quad (16)$$

The scale dependence of the \log^2 contribution requires that the coefficients C_s and C_u in Eq. (14) be scale dependent, and thus \tilde{C}_π becomes scale dependent and the scale dependence of \tilde{L}_5 is modified (a higher-order effect). The calculated values of \mathcal{F} , along with their uncertainties determined by jackknifing over the configurations, are shown in Table II and plotted in Fig. 3. We anticipate that the fit value of \tilde{L}_5 should change only a small amount from its value obtained in the NLO fits and in fit D, if the chiral expansion is convergent. However, we expect that the coefficient \tilde{C}_π could change by an amount of order 1. The results of fitting this functional form to the lattice data, which we denote by ‘‘Fit E,’’ are presented in Table IV and shown in Fig. 3 (error ellipse is shown in Fig. 4). Indeed, \tilde{L}_5 is changed very little, while \tilde{C}_π changes by an amount of order 1. We also give results for fits F and G which are the same as fit E except the argument of the \log^2 contribution is chosen to be $M = m_\pi$ and $M = m_K$, respectively. These choices lead to a larger variation in \tilde{L}_5 and consequently in f_K/f_π .

C. Discussion

To determine f_K/f_π at the physical point and its associated uncertainty we synthesize the results of the NLO and NNLO fits. Fitting the lowest two mass points at NLO gives $f_K/f_\pi = 1.215 \pm 0.002$, while fitting the three data points with pion masses below $m_\pi \sim 500$ MeV gives $f_K/f_\pi = 1.218 \pm 0.002$. The difference between them is within statistical errors (1.5σ) but there appears to be a systematic trend in the data which can be attributed to higher orders in the chiral expansion. As we are unable to fit the full NNLO expression to our small data set, we can estimate the systematic uncertainty in this calculation by looking at the range of values of f_K/f_π that result from the two types of NNLO extrapolation, both with and with-

out the \log^2 contribution, including variation in the argument of the NNLO logarithm and including statistical errors. The range of variation in the NNLO estimate is an order of magnitude larger than the statistical error found at NLO. We take this NNLO uncertainty, $\Delta(f_K/f_\pi) = {}^{+0.011}_{-0.022}$, to be an estimate of the systematic error in our calculation due to the truncation of the chiral expansion. We also assign a systematic error due to fitting procedures, obtained by varying the fitting ranges displayed in Fig. 1, which gives $\Delta(f_K/f_\pi) = {}^{+0.000}_{-0.010}$. Therefore, our final number on the MILC lattices with $b \sim 0.125$ fm is

$$\frac{f_K}{f_\pi} = 1.218 \pm 0.002 {}^{+0.011}_{-0.024}, \quad (17)$$

where the first error is statistical and the second error is systematic, with the extrapolation error and fitting error added in quadrature. The error in this lattice QCD determination of f_K/f_π is clearly dominated by the systematics.

Using a similar procedure, we arrive at a value for L_5 :

$$L_5(f_\pi^{\text{phy}}) = 5.65 \pm 0.02 {}^{+0.18}_{-0.54} \times 10^{-3}, \quad (18)$$

where the first error is statistical and the second is an estimate of the systematic error due to omitted higher orders in the chiral expansion. This then scales to give $L_5(m_\eta^{\text{phy}}) = 2.22 \pm 0.02 {}^{+0.18}_{-0.54} \times 10^{-3}$ at the η mass and $L_5(m_\rho^{\text{phy}}) = 1.42 \pm 0.02 {}^{+0.18}_{-0.54} \times 10^{-3}$ at the ρ mass. As stated previously, this is an effective L_5 as it includes the higher-order strange-quark contribution, and lattice-spacing artifacts.

The results for f_K/f_π have an additional systematic error due to the nonzero lattice spacing which we expect to be $O((m_s - m_u)b^2)$. In principle, one can reduce this error by fitting to the appropriate χ PT formulas that include the $O(g^2 b^2)$ effects through the use of lattice-spacing spurion fields, e.g. Ref. [24]. Such an analysis will account for all lattice-spacing effects arising at this order, including those due to flavor-symmetry breaking in the sea-quark sector, due to Lorentz-violating interactions arising from the lack of full Lorentz invariance on the lattice, and from lattice-spacing shifts to the coefficients of operators appearing in the chiral Lagrangian in the continuum limit. However, our data fit well to the continuum χ PT formulas and hence we do not expect that use of the extended χ PT formulas of Ref. [24] would significantly improve our results with our limited data set. Our final result at a lattice spacing of $b \sim 0.125$ fm, shown in Eq. (17), is consistent with the MILC number [1]

$$\left. \frac{f_K}{f_\pi} \right|_{\text{MILC}} = 1.210 \pm 0.004 \pm 0.013, \quad (19)$$

where the first error is statistical and the second is the total systematic error estimated by MILC. Since our valence quarks are domain-wall fermions, in contrast with the KS

quarks used by MILC, the discretization errors should be different. Hence, in the absence of a conspiracy or an accident, the agreement of our results to the few-percent level is further confirmation that these systematic errors due to a finite lattice spacing are small.⁶

It is also interesting to note that our result is in agreement with the experimental number,

$$\left. \frac{f_K}{f_\pi} \right|_{\text{exp}} = 1.223 \pm 0.012, \quad (20)$$

but our calculation has a somewhat larger systematic error due to uncertainty in the chiral extrapolation. To make a comparison with the experimental value, an estimate of the lattice-spacing error in our extraction is required. A naive estimate based upon the size of $b^2 \Lambda_{\text{QCD}}^2$ suggests that the systematic error associated with the lattice spacing is comparable to the systematic error associated with the truncation of the chiral expansion, $\sim \pm 0.02$.

It is possible to further improve the precision of our calculation by increasing the statistics of the lighter pion masses, including one more point at even lighter pion mass, and by better utilizing the power of partial quenching, i.e. by computing with different valence quark masses, away from the tuned point. We hope that with these improvements in place we will be able to improve upon the MILC result.

⁶A more recent MILC calculation [2] quotes a value of $1.198 \pm 0.003^{+0.016}_{-0.005}$. This calculation made use of finer lattices as well as a second run with a lighter strange-quark mass at $b \sim 0.125$ fm.

IV. CONCLUSIONS

Existing high-precision calculations of basic standard model quantities involve staggered valence quarks on staggered sea quarks with their associated systematic errors. Clearly, it is important to employ a variety of fermion discretizations in order to understand and reduce one of the inherent systematic errors in lattice QCD calculations. We have computed f_K/f_π with domain-wall valence quarks on MILC lattices with a lattice spacing of $b \sim 0.125$ fm and found results consistent with an earlier calculation by MILC using KS valence quarks. It is gratifying to find that using different fermions in the valence sector leads to a consistent precision determination of f_K/f_π in accord with basic effective field theory expectations about the scaling of discretization errors.

ACKNOWLEDGMENTS

This work was performed under the auspices of SciDAC. Useful discussions with C. Bernard are gratefully acknowledged. We thank R. Edwards for help with the QDP++/CHROMA programming environment [42] with which the calculations discussed here were performed. We are also indebted to the MILC and the LHP collaborations for use of some of their configurations and propagators, respectively. This work was supported in part by the U.S. Department of Energy under Grant No. DE-FG03-97ER4014 (M. J. S.), No. DF-FC02-94ER40818 (K. O.), No. ER-40762-365 (P. F. B.); the National Science Foundation under Grant No. PHY-0400231 (S. R. B.); and by DOE through Contract No. DE-AC05-84ER40150, under which the Southeastern Universities Research Association (SURA) operates the Thomas Jefferson National Accelerator Facility (K. O., S. R. B.).

-
- [1] C. Aubin *et al.* (MILC), Phys. Rev. D **70**, 114501 (2004).
 - [2] C. Bernard *et al.* (MILC), Proc. Sci., LAT2005 (2005) 025 [hep-lat/0509137].
 - [3] W. J. Marciano, Phys. Rev. Lett. **93**, 231803 (2004).
 - [4] M. Okamoto, Proc. Sci., LAT2005 (2005) 013 [hep-lat/0510113].
 - [5] P. B. Mackenzie *et al.* (Fermilab Lattice, MILC and HPQCD), Proc. Sci., LAT2005 (2006) 207.
 - [6] A. X. El-Khadra, A. S. Kronfeld, P. B. Mackenzie, S. M. Ryan, and J. N. Simone, Phys. Rev. D **64**, 014502 (2001).
 - [7] M. Okamoto *et al.*, Nucl. Phys. B, Proc. Suppl. **129**, 334 (2004).
 - [8] J. F. Lagae and D. K. Sinclair, Nucl. Phys. B, Proc. Suppl. **63**, 892 (1998).
 - [9] J. F. Lagae and D. K. Sinclair, Phys. Rev. D **59**, 014511 (1998).
 - [10] D. Toussaint and K. Orginos (MILC), Nucl. Phys. B, Proc. Suppl. **73**, 909 (1999).
 - [11] K. Orginos and D. Toussaint (MILC), Phys. Rev. D **59**, 014501 (1998).
 - [12] G. P. Lepage, Phys. Rev. D **59**, 074502 (1999).
 - [13] K. Orginos, D. Toussaint, and R. L. Sugar (MILC), Phys. Rev. D **60**, 054503 (1999).
 - [14] C. W. Bernard *et al.*, Phys. Rev. D **64**, 054506 (2001).
 - [15] C. Aubin and C. Bernard, Phys. Rev. D **68**, 034014 (2003).
 - [16] C. Aubin and C. Bernard, Phys. Rev. D **68**, 074011 (2003).
 - [17] D. B. Renner *et al.* (LHP), Nucl. Phys. B, Proc. Suppl. **140**, 255 (2005).
 - [18] R. G. Edwards *et al.* (LHPC), Proc. Sci., LAT2005 (2005) 056 [hep-lat/0509185].
 - [19] D. B. Kaplan, Phys. Lett. B **288**, 342 (1992).
 - [20] Y. Shamir, Phys. Lett. B **305**, 357 (1993).
 - [21] Y. Shamir, Nucl. Phys. **B406**, 90 (1993).

- [22] Y. Shamir, Phys. Rev. D **59**, 054506 (1999).
- [23] V. Furman and Y. Shamir, Nucl. Phys. **B439**, 54 (1995).
- [24] O. Bar, C. Bernard, G. Rupak, and N. Shoresh, Phys. Rev. D **72**, 054502 (2005).
- [25] J.-W. Chen, D. O'Connell, R. S. Van de Water, and A. Walker-Loud, Phys. Rev. D **73**, 074510 (2006).
- [26] S. R. Beane, P. F. Bedaque, K. Orginos, and M. J. Savage (NPLQCD), Phys. Rev. D **73**, 054503 (2006).
- [27] S. R. Beane, K. Orginos, and M. J. Savage, Nucl. Phys. **B768**, 38 (2007).
- [28] S. R. Beane, K. Orginos, and M. J. Savage, hep-lat/0604013.
- [29] C. W. Bernard *et al.* (MILC), Phys. Rev. D **66**, 094501 (2002).
- [30] S. Durr and C. Hoelbling, Phys. Rev. D **71**, 054501 (2005).
- [31] M. Creutz, hep-lat/0603020.
- [32] C. Bernard, Phys. Rev. D **73**, 114503 (2006).
- [33] C. Bernard, M. Golterman, Y. Shamir, and S. R. Sharpe, hep-lat/0603027.
- [34] S. Durr and C. Hoelbling, Phys. Rev. D **74**, 014513 (2006).
- [35] A. Hasenfratz and R. Hoffmann, Phys. Rev. D **74**, 014511 (2006).
- [36] C. Bernard, M. Golterman, and Y. Shamir, Phys. Rev. D **73**, 114511 (2006).
- [37] Y. Shamir, Phys. Rev. D **75**, 054503 (2007).
- [38] A. Hasenfratz and F. Knechtli, Phys. Rev. D **64**, 034504 (2001).
- [39] T. DeGrand, A. Hasenfratz, and T. G. Kovacs, Phys. Rev. D **67**, 054501 (2003).
- [40] T. DeGrand (MILC), Phys. Rev. D **69**, 014504 (2004).
- [41] S. Durr, C. Hoelbling, and U. Wenger, Phys. Rev. D **70**, 094502 (2004).
- [42] R. G. Edwards and B. Joo (SciDAC), Nucl. Phys. B, Proc. Suppl. **140**, 832 (2005).
- [43] C. McClendon, JLab Report No. JLAB-THY-01-29, 2001.
- [44] T. Blum *et al.*, Phys. Rev. D **69**, 074502 (2004).
- [45] Y. Aoki *et al.*, Phys. Rev. D **69**, 074504 (2004).
- [46] C. R. Allton *et al.* (UKQCD), Phys. Rev. D **70**, 014501 (2004).
- [47] L. Giusti, Proc. Sci., LAT2006 (2006) 009 [hep-lat/0702014].
- [48] J. Gasser and H. Leutwyler, Nucl. Phys. **B250**, 465 (1985).
- [49] J. Gasser and H. Leutwyler, Ann. Phys. (N.Y.) **158**, 142 (1984).
- [50] J. Gasser and H. Leutwyler, Phys. Lett. **125B**, 321 (1983).
- [51] S. Eidelman *et al.* (Particle Data Group), Phys. Lett. B **592**, 1 (2004).
- [52] G. Amoros, J. Bijnens, and P. Talavera, Nucl. Phys. **B568**, 319 (2000).
- [53] J. Bijnens, N. Danielsson, and T. A. Lahde, Phys. Rev. D **73**, 074509 (2006).
- [54] J. Bijnens, G. Colangelo, and G. Ecker, Phys. Lett. B **441**, 437 (1998).